SPE 134534

Practical use of well test deconvolution

Gringarten, A. C., SPE, Imperial College London

This paper was prepared for presentation at the 2010 SPE Annual Technical Conference and Exhibition held in Florence, Italy, 20–22 September 2010.

Abstract

Deconvolution transforms variable rate pressure data into a constant rate initial drawdown with a duration equal to the total duration of the test. It yields directly the corresponding pressure derivative, normalized to a unit rate. It is not a new interpretation method, but a new tool to process pressure and rate data in order to obtain more pressure data to interpret with conventional techniques.

Although deconvolution has received much attention since 2001 following the publication of a stable algorithm by von Schroeter, Hollaender, and Gringarten, its use by practicing engineers is still limited. One reason is limited access to the algorithm, which had only recently become available in commercial well test analysis software products. The other is concerns on how deconvolution should be used and how reliable it is. As a result, few examples of practical applications of well test deconvolution are available in the literature.

This paper illustrates various uses of deconvolution in tests of short and long durations. Examples include DST's with erroneous rates, which deconvolution is able to correct; and data from permanent downhole pressure gauges in vertical and horizontal wells, where deconvolution shows compartmentalization and recharge from other layers, which could not be seen in the original data.

Recommendations on how to perform deconvolution and how to verify deconvolution results are also provided. It is hoped that this paper will encourage well test interpreters to use deconvolution confidently as part of the well test analysis process.

Introduction

Deconvolution has received much attention in the past decade (von Schroeter *et al.* 2001, 2002, 2004; Gringarten *et al.* 2003; Levitan 2003; Levitan *et al.* 2004; Ilk *et al.* 2005, 2006; Amudo *et al.* 2006; Gringarten 2006; Whittle *et al.* 2008, 2009; Aluko and Gringarten 2009), following the publication of a stable deconvolution algorithm (von Schroeter *et al.* 2001). It is not a new interpretation method, but a new tool that processes pressure and rate data to obtain more pressure data to interpret. Deconvolution transforms variable-rate pressure data into a constant-rate initial drawdown with a duration equal to the total duration of the test, and yields directly the corresponding pressure derivative, normalized to a unit rate. This derivative is therefore free from distortions caused by pressure-derivative calculation algorithms, and from errors introduced by incomplete or truncated rate histories (Gringarten 2006). It also exhibits all the flow regimes that have been dominating throughout the test.

The Schroeter et al. (2001) deconvolution algorithm, based on the Total Least Square method, has been implemented, with some variations, in most commercial well test analysis softwares. Deconvolution is therefore readily available to all well test interpreters. Yet, by and large, its use seems to be mostly restricted to experts. One obvious reason is that the method is still new, and all new techniques take some time before they are adopted by practicing engineers (the well known "chasm", Moore 1991). This is not different from what happened when pressure type curve analysis was first introduced (Ramey 1970; McKinley 1971): it was suggested that it should be used only in emergency, after more conventional techniques had failed (Earlougher, 1977). Another reason is that the theoretical limitations of deconvolution and the difficulties that could be encountered using the deconvolution process have been over-emphasized. Moreover, shortcomings of particular software implementations have often been presented as limitations of deconvolution itself (as with derivatives in the mid-1980's).

This paper illustrates various uses of deconvolution in tests of short and long durations. Examples include DST's with erroneous rates, which deconvolution is able to correct; and data from permanent downhole pressure gauges in vertical and horizontal wells, where deconvolution shows compartmentalization and recharge from other layers, which could not be seen in from conventional analyses. Recommendations on how to perform deconvolution and how to verify deconvolution results are also provided. It is hoped that this paper will encourage well test interpreters to use deconvolution with confidence as part of their well test analysis process.

The deconvolution process

Algorithm

The deconvolution algorithm estimates both rates (called "adapted" rates herein) and rate-normalised derivative by minimising an error measure, *E*, which is a weighted combination of a pressure match, a rate match, and a penalty term based on the overall curvature of the graphed derivative, whose purpose is to enforce derivative smoothness (Eq. 1):

$$E = \left\| \left(p_i - y * g\right) - p \right\|_2^2 + \nu \left\| \left(y - q\right) \right\|_2^2 + \lambda \left\| \left(Dz - k\right) \right\|_2^2 \qquad (1)$$

In Eq. 1, p and q are the measured pressure and rate data, respectively; p_i is the initial pressure at the start of the rate history, which can be an input into or an output from deconvolution; $\left\| Dz - k \right\|_2^2$ is the curvature measure; λ and ν are weights for the rate match and the curvature, normalized to the weight for the pressure match (different well test analysis softwares define λ and ν differently); y is the adapted rate; and g is the instantaneous source function (Gringarten and Ramey, 1973), i.e. the derivative of the pressure with respect to time. Both y and g are outputs of deconvolution.

Actually, *t.g(t)*, the derivative of the pressure with respect to the natural log of time, is calculated instead of *g(t)*: an arbitrary shape of *t.g(t)* is input as an initial guess into Eq.1, and it is modified in successive iterations until the error mesure *E* is minimized (Fig. 1). The result is the deconvolved derivative.

Deconvolution is in principle only valid for linear systems, i.e. reservoirs with a slightly compressible fluid (in practice, deconvolution can be used with pseudo-pressures in the case of gas or multiphase flow). A further assumption is that the pressure is uniform in the reservoir at the start of the rate history.

Deconvolution could be performed on a single flow period[1], several flow periods, or part or all of the pressure history. The resulting deconvolved derivative is defined piecewise: in the case of a single flow period, it reproduces the flow period derivative at early times (as it would appear for the very first drawdown in the reservoir after pressure stabilisation). At later times, it is defined only from the start to the end of the flow period, as measured from the start of the test. It is interpolated between the two. In the case of multiple flow periods, on the other hand, the early part of the deconvolved derivative is some average of the derivatives for each flow period, and the later part is defined only from the start to the end of each flow period. The complete deconvolved derivative is again obtained by interpolation. The "average" at early times may be different from any of the original flow period derivatives, if changes have occured, for instance, in skin effects or wellbore storage coefficients. It could also be polluted by noise from some of the deconvolved flow periods, such as phase redistribution in the wellbore. This is not too much of a concern, as the primary objective of deconvolution is to generate data beyond what is available in individual flow periods (yellow bands in Fig. 2). Data already available in a particular flow period can be analysed by conventional means.

In practice, one tends to deconvolve individual build ups, or groups of build ups, or continuous ranges of pressure history. Drawdowns are often too noisy to be deconvolved individually.

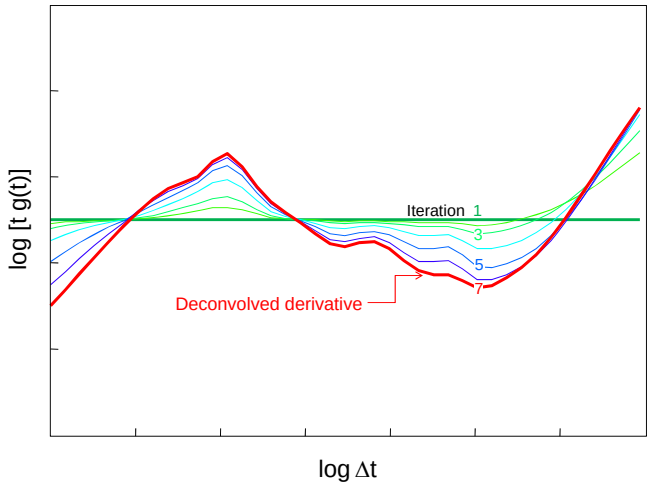

Figure 1: Iterative calculation of deconvolved derivative

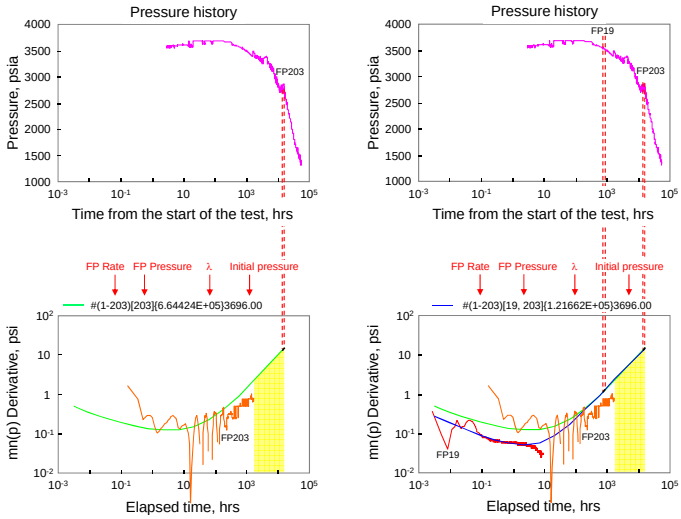

Figure 2: Well 1: Construction of the deconvolved derivative

The construction of the deconvolved derivative is illustrated in Fig. 2 with test data from Well 1 (Figs. 3 and 4). Well 1 has been drilled horizontally in the upper layer (Zone 1) of a two-layer gas condensate reservoir with a two-meter thick shale layer separating Zone 1 from Zone 3 (Fig. 3). Deconvolved derivatives in Fig. 2 and in this paper are identified by a label which describes the conditions of the deconvolution:

- (…..) refers to the rate record used. For instance, (1-203) means that the rate history with 203 different rates has been used.

[1] In this paper, a flow period (FP) refers to a period at constant rate, which could be a drawdown or a build up.

- […..] identifies the pressure data that have been deconvolved: [19] and [203] means that only the data from FP19 and FP203 were involved. [1-203] corresponds to the deconvolution of the entire pressure history up to the end of FP203 (Figs. 6 to 9).
- {….} states the value of the regularisation parameter λ
- The last parameter in the label represents the initial pressure $(p_{av})_i$

The left hand side of Fig. 2 shows the deconvolved derivative for a single flow period, FP203, a 1785 hour build up from 14500 hours to 16384 hours of production. The vertical axis is labeled in terms of normalized pseudo-pressure, a modification of the single-phase pseudo-pressure function used to linearize the diffusivity equation in gas reservoirs (Meunier *et al.* 1987). The deconvolved derivative is defined by the derivative of FP203 from 0 to about 100 hours, and by FP203 between 14500 hours and 16384 hours. The difference between the deconvolved derivative and the actual FP203 derivative in the 100 to 1785 hour range is due to the fact that the former is a drawdown derivative, corresponding to the first drawdown after stabilization, whereas the latter is a multirate derivative, which is affected by the rate history when boundaries have been reached.

The right hand side of Fig. 2 shows the deconvolved derivative for both FP19 and FP203. FP19 is an 11 hour build up between 809 hours and 820 hours, during the DST. The deconvolved derivative is a combination of the FP19 and FP203 derivatives from 0 to 1785 hours, and is defined by FP19 between 809 hours and 820 hours and by FP203 between 14500 hours and 16384 hours. In this particular example, FP19 and FP203 do not overlap: FP19 is infinite acting and dominates at early and middle times, whereas FP203 has boundary effects and dominates at late times. The yellow bands in Fig. 2 represent the increase in the radius of investigation, one full log-cycle in this case.

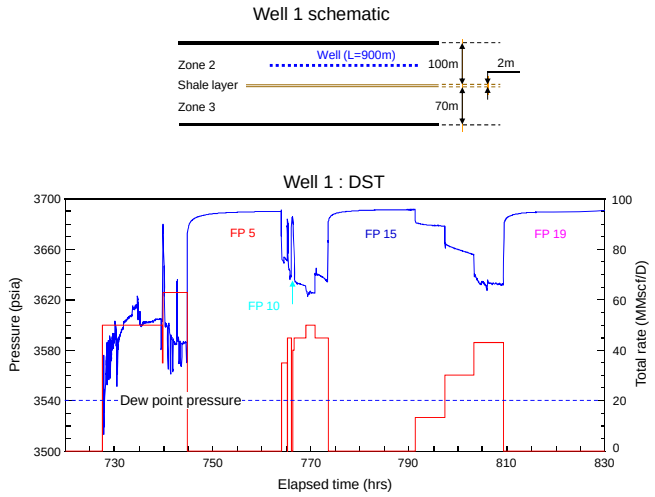

Figure 3: Well 1: DST

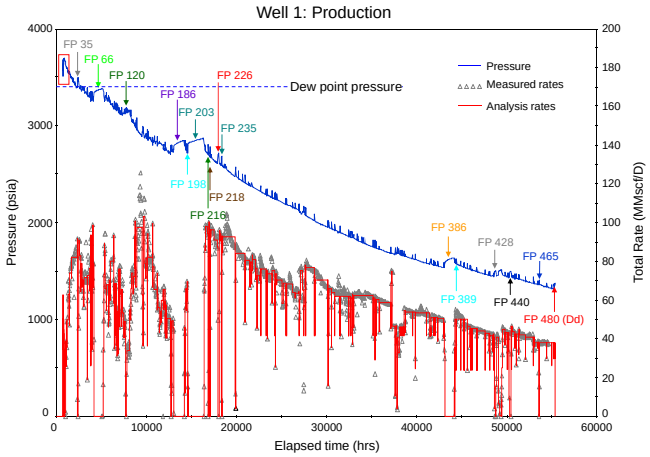

Figure 4: Well 1: production history

Control parameters

Deconvolution weight parameters

The estimate E in Eq. 1 depends on two weights, ν for the rate match, and λ for the roughness penalty. ν is set at a default value, $\nu_{def} = \frac{N}{m}\frac{\|\Delta p\|_2^2}{\|q\|_2^2}$, where Δp is the vector of pressure drop data, q is the vector of measured rates, m is the number of pressure points and N is the number of flow periods (von Schroeter *et al.* 2004). In the case of the deconvolution of a single flow period, λ is also set at a default value, $\lambda_{def} = \frac{\|\Delta p\|_2^2}{m}$. For multiple flow period deconvolution, λ must usually be set at 10 to 100 times λ_{def} to avoid oscillations on the derivative. Regularisation introduces bias, and thus the user must choose a level of λ that imposes just enough smoothness to eliminate small-scale oscillations on the deconvolved derivative while preserving genuine reservoir features. This is illustrated in Fig. 5 for the deconvolution of Well 1 pressure history from the start of the test to the end of FP203. Oscillations that exist at middle times in the deconvolved derivative for the λ_{def} value of $4.41231.10^4$ increase as λ decreases to $\lambda_{def}/10$ and decrease as λ increases to 10 λ_{def} and 100 λ_{def}. All the derivatives converge at late times, suggesting a satisfactory deconvolution in all cases.

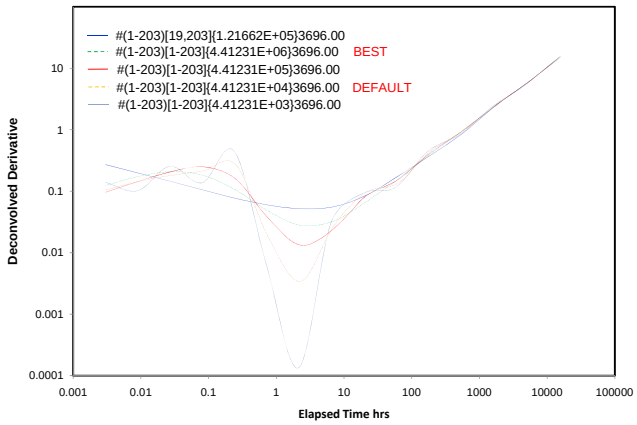

Figure 5: Impact of λ on deconvolution of an entire pressure history

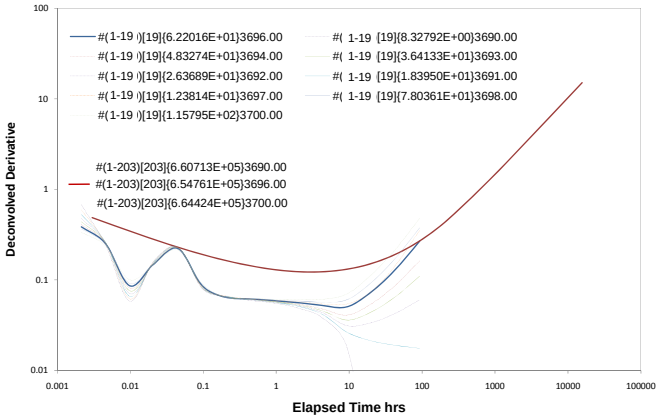

Figure 7: Impact of p_i on deconvolution

Initial pressure

The deconvolved derivative is very sensitive to the initial pressure if the flow period being deconvolved is infinite acting, and not sensitive if boundaries have been reached. This is illustrated in Fig. 7, which shows different shapes of FP19 deconvolved derivatives for different values of p_i. The FP203 derivatives, on the other end, are not affected. A good estimate of the initial reservoir pressure is therefore required, which can be obtained from a preliminary analysis of the data. Alternatively, p_i can be obtained by trial and error if at least two different, infinite acting build ups are available, as a correct p_i must yield the same deconvolved derivative (Levitan *et al.*, 2004). This is shown in Fig. 8 for FP15 and FP19, the last two DST build ups: an initial pressure of 3696 psia yields almost identical deconvolved derivatives.

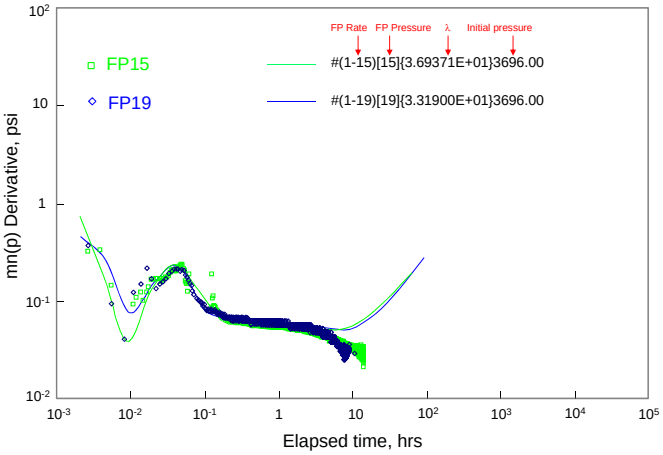

Figure 8: Well 1: Verification of p_i

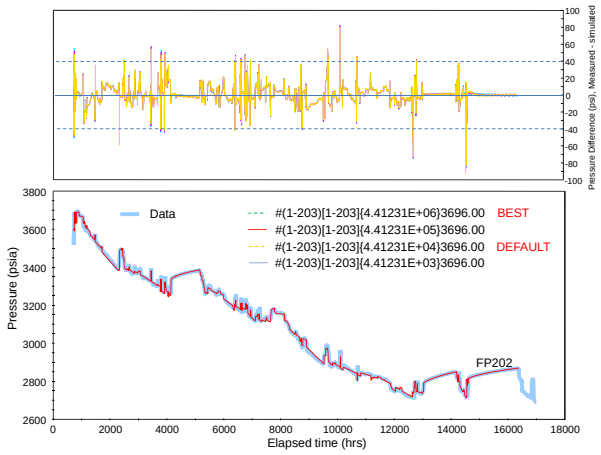

Figure 9: Well 1: Pressure history match

Verification of deconvolution

Deconvolution quality is assessed by the lack of late time oscillations on the deconvolved derivatives; by the fact that different flow periods yield converging derivatives (as in Fig. 5); and by the consistency between the deconvolved derivatives and possible interpretation models resulting from a conventional analysis of the data. A further and most important check is the ability to generate a pressure history from the deconvolved derivative that matches the actual pressure history. Such a match is shown in Fig. 9 for the deconvolved derivatives of Fig. 5. All deconvolved derivatives yield a satisfactory match with actual pressure data, with maximum errors of less that 10% in the drawdowns.

Interpretation methodology using deconvolution

The methodology for well test analysis using deconvolution is illustrated in Fig. 10. Pressure and rate data are deconvolved using appropriate values of the weight parameters ν and λ. For a gas well, pressure data are converted to pseudo-pressure or normalised pseudo-pressure in order to approximate a linear system before applying deconvolution. Once a satisfactory derivative has been obtained, a convolved pressure history is calculated from that derivative, the adapted rates and the initial pressure obtained from or used in deconvolution, and compared with the measured pressure history. If the match is acceptable, the deconvolved derivative is used to generate a unit-rate pseudo-pressure drawdown which has the same duration of that of the entire test. This unit-rate drawdown is analysed in the conventional way. The resulting model is then applied to the measured pressure data using the adapted rates, and the model parameters are refined until an acceptable match is obtained.

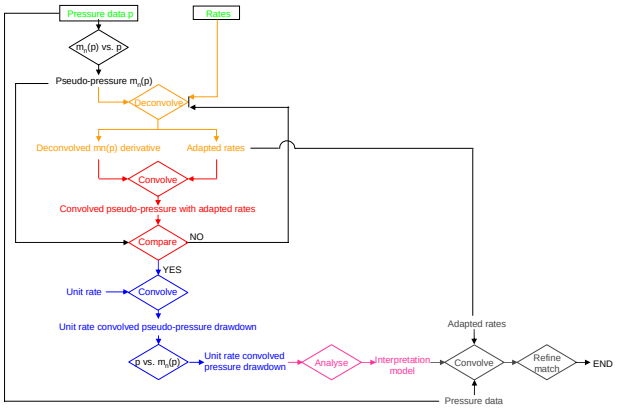

Figure 10: Deconvolution interpretation methodology (Amudo *et al.* 2006)

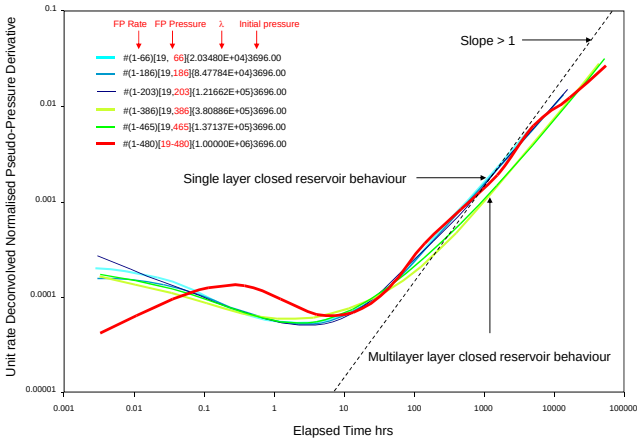

Figure 11: Well 1 deconvolved derivatives

Identification of boundaries and connectivities not visible by conventional analyses

One primary advantage of deconvolution is in the increase of the radius of investigation, which allows seeing reservoir features not visible in individual flow periods. Examples can be found in Gringarten (2006) and Aluko and Gringarten (2009). This is further illustrated here with Well 1 in Figs. 11 to 14, using the methodology described by Fig. 10. In the log-log plot of Fig. 11, production build ups (FP66, 185, 203, 386, 465 and 480) are deconvolved together with FP19 to add early time data to the deconvolved derivatives. All deconvolved derivatives exhibit unit slope log-log straight lines at late times, indicating a closed reservoir[2]. The late time unit-slope log-log straight lines for the later build ups (FP386 and 465) merge into a single straight line which is shifted to the right compared to the merged unit-slope log-log straight line for the first one year and a half of production (FP66, 186 and 203), indicating an increased drainage volume.

Fig. 11 also shows the deconvolved derivative of all pressure data from FP19 to FP481 (the quality of this derivative is verified in Fig. 12). At late times, it first follows the unit-slope straight line corresponding to FP66, 186 and 203, and then trends toward that for FP386 and 440. This suggests a multilayered behaviour due to drainage of Zone 3 through the shale layer. The transition occurs around 5000 hours and cannot be seen on any of the individual build ups or drawdowns.

The unit-rate drawdown convolved from the FP19-480 deconvolved derivative is analysed with a 3-layer closed reservoir model in Fig. 13. The top, middle and bottom layers represent Zone 2, the shale layer, and Zone 3, respectively. The FP19 to 481 multilayer behaviour is matched with a shale layer vertical permeability of 10^{-4} mD. The reservoir is a closed rectangle, with boundaries at distances of approximately 300m, 2200m, 400m and 800m.

As a final step, the multilayer model is applied to actual production build ups and the corresponding analysis parameters are adjusted as required to improve the match (Fig. 14).

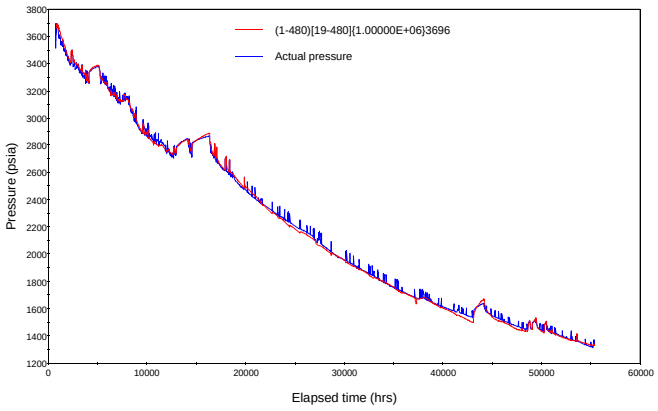

Figure 12: Well 1: verification of FP19-480 deconvolution

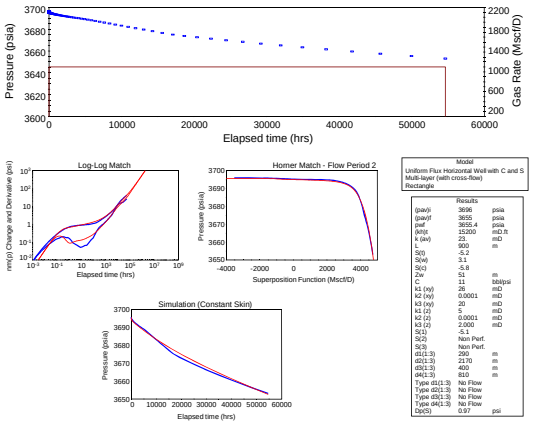

Figure 13: Well 1: Analysis of the unit rate drawdown generated from FP19-480 deconvolved derivative

[2] The straight line slope is not exactly one because of non-linearity due to gas flow, as observed by Levitan and Wilson (2010) who propose a correction based on material balance. The slope is close enough to one, however, so that a closed system can be diagnosed without ambiguity.

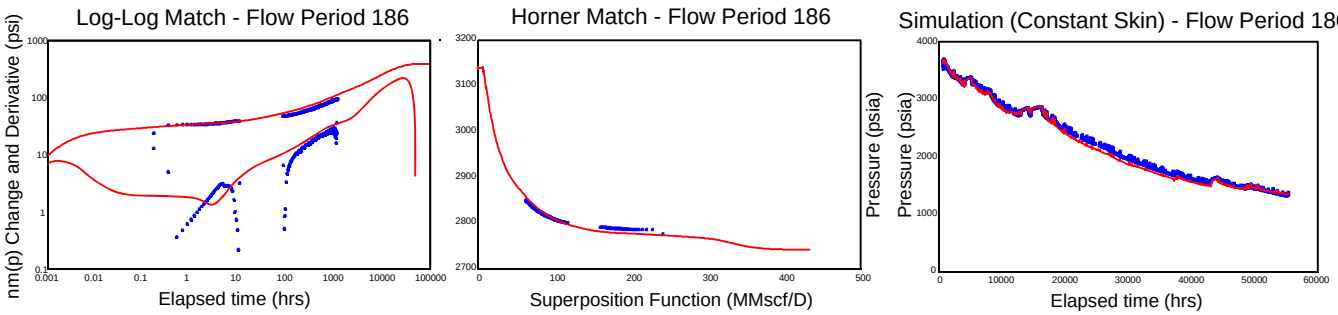

Figure 14: Well 1: analysis of build up FP186 with the interpretation model from the unit-rate drawdown analysis

Correction of rates

Another use of deconvolution is in correcting erroneous rates or determining missing rates. This is achieved by deconvolving the entire rate history and adapting the entire rate history.

Test with erroneous rates

Rate correction is illustrated with the test for oil Well 2 shown in Fig. 15. The test includes a number of drawdowns and build ups, with the two main build ups identified as FP12 and FP39. Rates are clearly not consistent with the pressure trend, especially during the main drawdown between 320 and 375 hours. The rate inconsistencies are confirmed in the rate-normalised log-log plot in Fig. 16. On this plot, the derivatives for the first and second build ups, FP12 and FP39, show stabilisations after 5 hours which could correspond to radial flow. The different stabilisation levels could imply a variation of permeability during the test. More likely, they indicate errors in the rate measurements. These rate errors can be corrected by deconvolution.

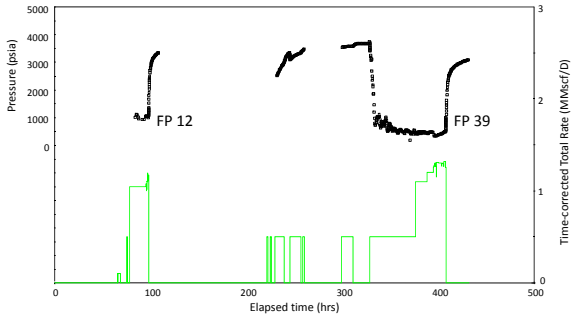

Figure 15: Well 2: Pressure and rate histories

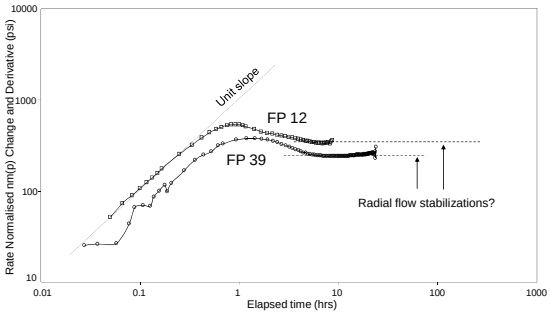

Figure 16: Well 2: Rate normalized log-log plot

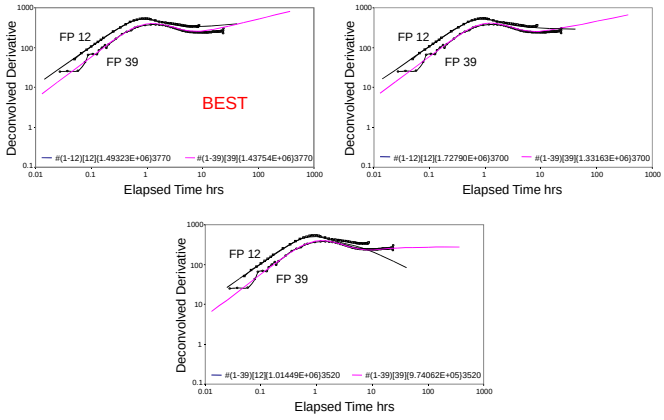

Figure 17: Well 2: Determination of p_i

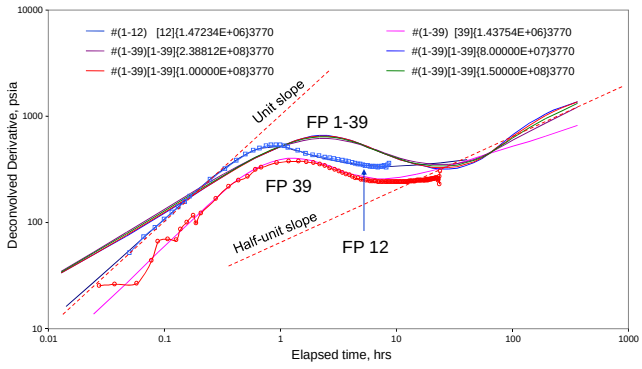

Figure 18: Well 2; Deconvolution with p_i = 3770 psia

The initial pressure for deconvolution is determined by trial and error, according to the procedure described by Levitan et al. (2004). The deconvolved derivatives for the two build ups, calculated for a range of p_i values based on RFT measurements, are compared in Fig. 17: the deconvolved derivatives must coincide at late times for p_i to be correct; otherwise, they diverge or cross. The best estimate from Fig. 17 (3770 psia) is then used to deconvolve the entire pressure history (FP1-39 in Fig. 18). Several λ values are tried to obtain the "best" deconvolved derivative, which corresponds to $\lambda = 1.5\ 10^8$. It has a duration of 366 hours, which is the duration of the entire test, whereas the duration of the longest build up is 24 hours only. The quality of the deconvolution is verified in Fig. 19 by comparing the pressure history calculated from the deconvolved derivative of FP1-

39 with the actual pressure measurements. The match is reasonably good for all the values of λ used in the deconvolution.

The rates corrected by deconvolution of FP1-39 are shown in Fig. 20 (continuous lines). Although they slightly differ for different values of λ, they all show the same overall trend and are different from the reported rates (dashed line), except where the rates have actually been measured. The corresponding rate-normalised log-log plot is shown in Fig. 16. Contrary to rate-normalised log-log plot in Fig. 11, this plot now shows good consistency between FP12 and FP39.

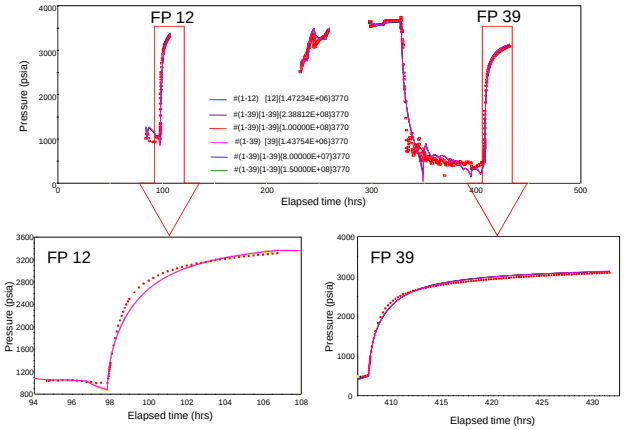

Figure 19: Well 2: Verification of deconvolution

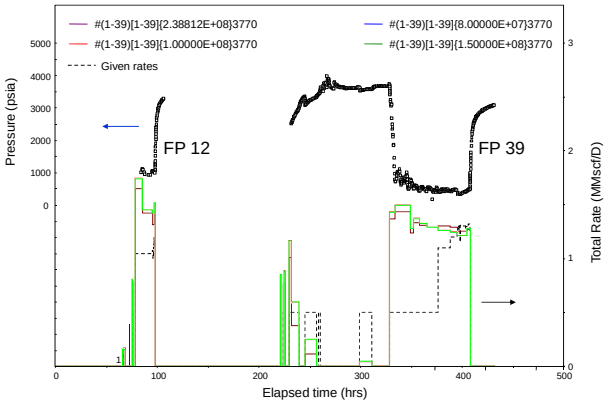

Figure 20: Well 2: Adapted rates

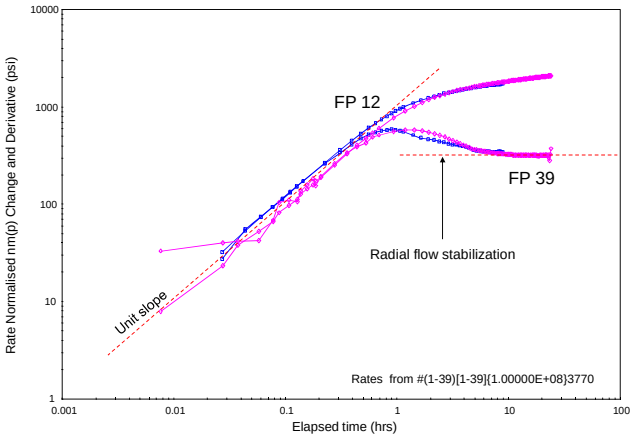

Figure 21: Well 3: Adapted rate normalized log-log plot

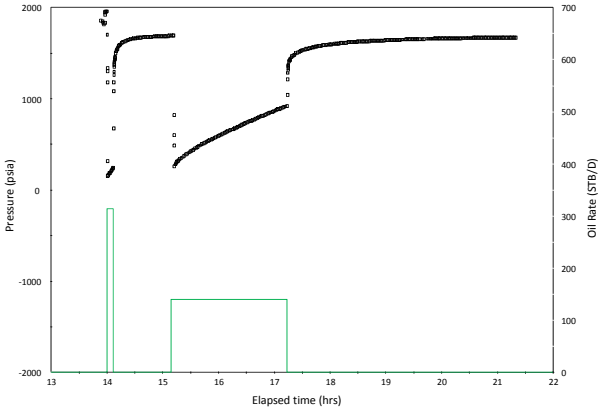

Figure 22: Well 3: Pressure and rate histories

DST with increasing liquid level during drawdowns

Fig. 22 shows the rate and pressure histories for a DST in oil Well 3. The pressure increases during the drawdowns, which indicates a liquid level in the well. The rates are reported as constant during the drawdowns, which is incorrect. The usual procedure is to convert pressures into fluid levels and use these to calculate the actual rates. Alternatively, rates can be obtained by deconvolution.

To that end, the first and second drawdowns are divided into 4 and 12 different periods at constant rate, respectively, prior to deconvolving the entire pressure history with rate adaptation. Results are shown in Fig. 23. For comparison, deconvolved derivatives for the two build ups, FP7 and 21, and for the entire pressure history without rate adaptation are also included. The default λ value for deconvolving the entire history is $3.68106\ 10^5$ with and without rate adaptation. λ has to be increased to 10^6 with rate adaptation and to $3.68106\ 10^7$ without rate adaptation to eliminate oscillations. The resulting deconvolved derivatives are only slightly different. The pressure histories calculated from the deconvolved derivatives, with and without rate adaptation, are compared to the actual pressure history in Fig. 24. With the adapted rates also shown in Fig. 4, the match is good. Without rate adaptation, only the build ups are matched.

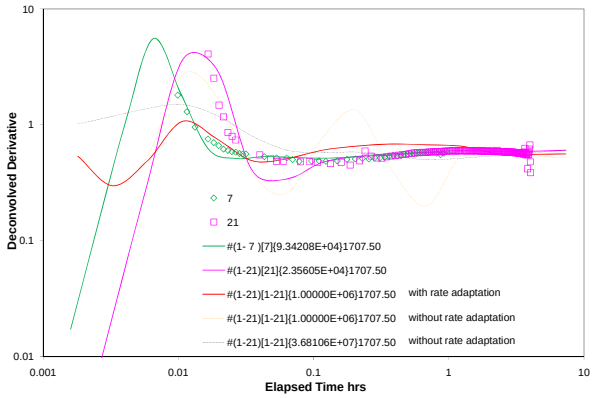

Figure 22: Well 3: Deconvolved derivatives

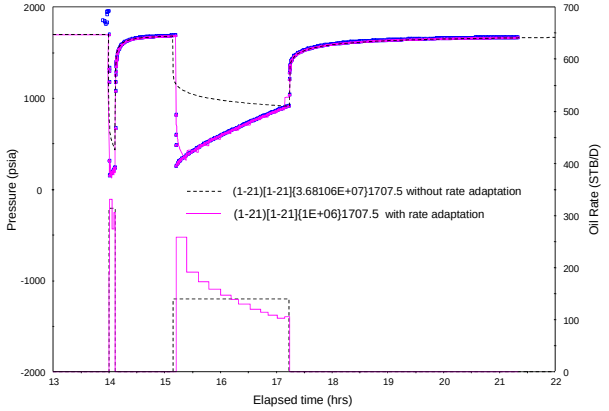

Figure 23: History pressure matches with and without rate adaptation

Although unlikely in the particular case of Well 3 DST, the increase in drawdown pressure could also be attributed to a decrease in skin effect. In the same way, deconvolution cannot distinguish an error in rate from a change in skin factor. It is up to the interpreter to make this distinction.

Discussion and Conclusion

This paper has presented examples for two main benefits of deconvolution: (1) access to radius of investigation of the entire test, which allows seeing boundaries and connectivities not visible in individual flow periods; and (2) the correction of erroneous rates and the determination of missing rates. Both require applying deconvolution to entire pressure history sequences, including build up and drawdown data.

Although deconvolution is theoretically only valid for linear systems, it can be applied to systems that are pseudo-linear, such as with gas and multiphase flow. As any other interpretation method, such as straight lines and derivatives, it cannot be used blindly, but requires knowledge and intuition from the user. In particular, the validity of the deconvolution must be established, by verifying that the pressure history calculated from the deconvolved derivative can closely reproduce the actual pressure measurements.

Nomenclature

D	matrix in curvature measure
E	error measure
FP	flow period
g	instantaneous source function
k	vector in curvature measure
m	number of pressure points
N	number of flow periods
p	vector of measured pressure
p_i	initial pressure, psia
q	vector of measured rate
t	time
y	vector of adapted rate
z	coefficient of the deconvolved derivative
λ	regularization parameter
ν	rate error weight
λ_{def}	default value of regularization parameter
ν_{def}	default value of rate error weight
Δp	vector of pressure drop data
$nm(p)$	normalized pseudo-pressure $\left(\frac{\mu Z}{2p}\right)\int_{p_0}^{p}\frac{2p}{\mu Z}dp$ $psia$

References

1. Aluko, O.A. and Gringarten, A.C., 2009:" Well Test Dynamics in Rich Gas Condensate Reservoirs under Gas Injection," paper SPE 121848 presented at the 2009 SPE EUROPEC/EAGE Annual Conference and Exhibition held in Amsterdam, The Netherlands, 8–11 June.
2. Amudo C., Turner, J., Frewin J.; Kgogo, T., and Gringarten A. C., 2006:"Integration of Well Test Deconvolution Analysis and Detailed Reservoir Modelling in 3D Seismic Data Interpretation: A Case Study," paper SPE 100250 presented at the SPE Europec/EAGE Annual Conference and Exhibition, Vienna, Austria, 12–15 June
3. Earlougher, R.C. Jr., 1977. *Advances in Well Test Analysis*, Monograph Series. Richardson, Texas: SPE, **5.**
4. Gringarten A. C., 2006:" From Straight lines to Deconvolution: the Evolution of the State of the art in Well Test Analysis," paper SPE 102079, presented at the 2006 SPE Annual Technical Conference and Exhibition, San Antonio, Texas, U.S.A., 24–27 September 2006; SPEREE (Feb. 2008) 11-1 pp. 41-62.
5. Gringarten, A. C., von Schroeter, T., Rolfsvaag, T., and Bruner, J., 2003:"Use of Downhole Pressure Gauge Data to Diagnose Production Problems in a North Sea Horizontal Well," paper SPE 84470, presented at the 2003 SPE Annual Technical Conference and Exhibition, Denver, CO, Oct. 5 – Oct. 8.
6. Ilk, D., Anderson, D. M., Valko, P. P., and Blasingame, T. A., 2006: "Analysis of Gas-Well Reservoir Performance Data Using B-Spline Deconvolution," paper SPE 100573 presented at the Gas Technology Symposium, Calgary, Alberta, Canada, 15-17 May, 2006.
7. Ilk, D., Valkó, P.P. and Blasingame, T.A., 2005:"Deconvolution of Variable Rate Reservoir Performance Data Using B-Splines," paper SPE 95571 presented at the 2005 SPE Annual Technical Conference and Exhibition, Dallas, Tx, 9-12 Oct. 2005.
8. Levitan, M. M., 2003:"Practical Application of Pressure-Rate Deconvolution to Analysis of Real Well Tests", paper SPE 84290, presented at the 2003 SPE Annual Technical Conference and Exhibition, Denver, CO, Oct. 5 – Oct. 8.
9. Levitan, M. M., Crawford, G. E., and Hardwick, A., 2004:" Practical Considerations for Pressure-Rate Deconvolution of Well Test Data," paper SPE 90680 presented at the SPE Annual Technical Conference and Exhibition held in Houston, Texas, U.S.A., 26–29 September.

10. Levitan, M.M. and Wilson, M.R., 2010:" Deconvolution of Pressure and Rate Data From Gas Reservoirs With Significant Pressure Depletion," paper SPE 134261 presented at the 2010 Annual Conference and Exhibition held in Florence, Italy, 19-22 September
11. McKinley, R.M., 1971:"Wellbore transmissibility from Afterflow-Dominated Pressure buildup Data," J. Pet. Tech. (Jan 1971)
12. Meunier, D.F., Kabir, C.S., and Wittmann, M.J.,1987. Gas Well Test Analysis: Use of Normalized Pressure and Time Functions. *SPEFE* **2** (4): 629–636. SPE-13082-PA. DOI: 10.2118/13082-PA.
13. Moore, G., 1991: *Crossing the Chasm*, HarperCollins Publishers Limited ISBN 0-06-051712-3
14. Ramey, H.J., Jr., 1970:"Short-Time Well test Data Interpretation in the Presence of Skin Effect and Wellbore Storage," J. Pet. Tech. (Jan 1970) 97.
15. von Schroeter, T., Hollaender, F., and Gringarten, A. C., 2001: "Deconvolution ofWell Test Data as a Nonlinear Total Least Squares Problem," paper SPE 71574 presented at the 2001 SPE Annual Technical Conference and Exhibition, New Orleans, Louisiana, 30 September – 3 October; SPEJ (Dec. 2004) pp. 376-390.
16. von Schroeter, T., Hollaender, F., Gringarten, A., 2002:"Analysis of Well Test Data From Permanent Downhole Gauges by Deconvolution," paper SPE 77688, presented at the 2002 SPE Annual Technical Conference and Exhibition, San Antonio, TX, Sept. 29 – Oct. 2.
17. Whittle, T. and Gringarten A. C., 2008:" The Determination of Minimum Tested Volume from the Deconvolution of Well Test Pressure Transients," paper SPE 116239, presented at the 2008 SPE Annual Technical Conference and Exhibition, Denver, Co., U.S.A., 21–24 September.
18. Whittle, T., Jiang, H., Young, S. and Gringarten A. C., 2009:"Well Production Forecasting by Extrapolation of the Deconvolution of the Well Test Pressure Transients," paper SPE 122299 presented at the 2009 SPE EUROPEC/EAGE Annual Conference and Exhibition held in Amsterdam, The Netherlands, 8–11 June.